Received: 22 March 2024 | *Revised:* 10 May 2024 | *Accepted:* 24 May 2024
DOI: 10.37917/ijeee.21.1.14 *Early View* | *June 2025*

Iraqi Journal for Electrical and Electronic Engineering
Original Article

Open Access
IJEEE University of Basrah College of Engineering

Advanced Neural Network-Based Load Frequency Regulation in Two-Area Power Systems

Mohammed Taha Yunis*[1], Mohamed DJEMEL[2]
[1]University of Sfax, National Engineering School of Sfax, Control an Energy Management Laboratory (CEMLab), Iraq
[2]University of Sfax, National Engineering School of Sfax, Control an Energy Management Laboratory (CEMLab), Tunisia

Correspondance
*Mohammed Taha Yunis
Iraq-Thi qar
Email: mohammed.taha@stu.edu.iq

Abstract
In this paper, enhancing dynamic performance in power systems through load frequency control (LFC) is explored across diverse operating scenarios. A new Neural Network Model Predictive Controller (NN-MPC) specifically tailored for two-zone load frequency power systems is presented. " Make your paper more scientific. The NN-MPC marries the predictive accuracy of neural networks with the robust capabilities of model predictive control, employing the nonlinear Levenberg-Marquardt method for optimization. Utilizing local area error deviation as feedback, the proposed controller's efficacy is tested against a spectrum of operational conditions and systemic variations. Comparative simulations with a Fuzzy Logic Controller (FLC) reveal the proposed NN-MPC's superior performance, underscoring its potential as a formidable solution in power system regulation.

Keywords
Neural Network Model Predictive Control (NN-MPC), Load Frequency Control (LFC), Power System Regulation, Dynamic Performance Enhancement, Levenberg-Marquardt Optimization,Two-zone Power System Nonlinear optimization.

I. Introduction

Large-scale power systems typically consist of multiple interconnected sub-systems, each linked by tie-lines. Control areas, equipped with one or more generators, are tasked with managing their own demand and power exchanges with adjacent regions [1]- [2]. Given the fluctuating nature of power system loads, load frequency controllers are essential to sustain system frequency at its nominal value [3]- [4] . It is understood that variations in real power primarily influence system frequency, and mechanical power input to generators is pivotal for regulating the frequency of the electrical output. In the context of a deregulated power system, control areas are subject to a range of uncertainties and disturbances due to increased complexity, errors in system modeling, and evolving power system configurations [5]- [6]. An effectively designed and managed power system must adapt to load changes and disturbances [7]. delivering high-quality power while keeping voltage and frequency within acceptable bounds [8]- [9]. Over the past few decades, a Plethora of control strategies for Load Frequency Control (LFC) has emerged, as highlighted in the literature [10]– [11]. This surge of interest stems from LFC's critical role in power system operations, its primary goal being the regulation of generator output to set levels while maintaining frequency fluctuations within predetermined limits. Advanced robust adaptive control frameworks [12]. Have been formulated to address LFC's system parameter variations. Innovative algorithms [13], have enhanced multi-area power system operations, while decentralized control designs for multi-input multi-output systems [14]. Have shown that a cohort of local controllers can ensure systemic stability and performance. The significance of robustness and stability in LFC design is evident in findings from [15]- [16], and practical considerations concerning current utility technologies and hybrid LFC structures are discussed in [17]- [18] . The integration

of artificial neural networks, genetic algorithms, fuzzy logic, and optimal control into LFC is well-documented [19]– [20]. Model Predictive Control (MPC), a mainstay in industrial applications, relies on process models to forecast plant behavior, distinguishing itself by incorporating constraints for tighter control and reliability 17–18. Variants of MPC, such as Model Algorithmic Control (MAC), Dynamic Matrix Control (DMC) [21], and Internal Model Control (IMC) [22], share a fundamental reliance on linear process modeling. Neural Network Model Predictive Control (NN-MPC) represents a direct application of neural networks to nonlinear control, where the neural network serves as a predictive model for process output [23]. While NN-MPC has seen application in fields like chemical and industrial processes [24] its adoption in power system stability and control remains nascent [25]. This study delves into the deployment of an NN-MPC for addressing the LFC and inter-area tie-power control challenges within a multi-area power system [26]. Through rigorous modeling and simulation, the NN-MPC's design and implementation are explored. Comparative analyses with A Fuzzy Logic Controller (FLC) under diverse conditions substantiate the NN-MPC's feasibility and superior efficacy [27]. The simulation outcomes affirm the proposed controller's enhanced performance capabilities, with NN-MPC showing considerable promise in improving system response [28]

II. Load-Frequency Control (LFC) Across a Two-Area Power System

Figure 1 presents a schematic of the area within an *n*-area power system, employing a linearized model suitable for minor load variations typical of regular operations. This approach simplifies the load-frequency control analysis. For the study at hand, we consider an interconnected two-area load-frequency control system, depicted in Figure 2. The model's governing equations, which are integral to the two-area load-frequency control, are enumerated as follows:

$$P_{G1} = \frac{-1}{T_{G1}}\Delta P_{G1} + \frac{-1}{R_1 T_{G1}}\Delta f_1 + \frac{1}{T_{G1}}u_1 \tag{1}$$

$$\dot{P}_{T1} = \frac{1}{T_{T1}}\Delta P_{G1} - \frac{1}{T_{T1}}\Delta P_{T1} \tag{2}$$

$$\dot{f}_1 = K_{p1}\frac{1}{T_{p1}}\Delta P_{T1} - \frac{1}{T_{p1}}\Delta f_1 - K_{p1}\frac{1}{T_{p1}} \tag{3}$$

$$\dot{P}_{tie} = T_{12}\Delta f_1 - T_{12}\Delta f_2 \tag{4}$$

$$\dot{P}_{G2} = -\frac{1}{T_{G2}}\Delta P_{G2} + \frac{1}{R_2 T_{G2}}\Delta f_2 + \frac{1}{T_{G2}}u_2 \tag{5}$$

$$\dot{P}_{T2} = \frac{1}{T_{T2}}\Delta P_{G2} - \frac{1}{T_{T2}}\Delta P_{T2} \tag{6}$$

$$\dot{f}_2 = K_{p2}\frac{1}{T_{p2}}\Delta P_{T2} - \frac{1}{T_{p2}}\Delta f_2 - a_{12}K_{p2}\frac{1}{T_{p2}}\Delta P_{tie} - K_{p2}\frac{1}{T_{p2}}\Delta P_{d2} \tag{7}$$

In a two-area power system, the dynamic behavior can be described using the following terms:

$\dot{f}_i$: Incremental frequency deviation in the *i*th area.
ΔP_{di} : Incremental change in load demand in the *i*th area.
ΔP_{tie} : Incremental change in tie-line power.
ΔP_{Gi} : Incremental change in governor position for the *i*th area.
ΔP_{Ti} : Incremental change in power generation level for the *i*th area.
B_i : Frequency bias constant for the *i*th area.
T_{Gi} : Governor time constant for the *i*th area.
T_{Ti} : Turbine time constant for the *i*th area.
K_{pi} : Power system gain for the *i*th area.
T_{pi} : Power system time constant for the *i*th area.
T_{ij} : Synchronizing constant between the *i*th and *j*th areas.

The dynamic model of this two-area power system can be succinctly represented in a state-space form as follows:

$$\dot{x} = Ax + Bu + d \tag{8}$$

In this representation, x is the state vector, A and B are system matrices, u is the control input vector, and dd is the disturbance vector. This framework allows for a comprehensive analysis of the system dynamics, facilitating the understanding and design of control strategies for effective power system management.

$$\dot{x} = Ax + Bu + d$$

$$x = \begin{bmatrix} \Delta P_{G1} \\ \Delta P_{T1} \\ \Delta f_1 \\ \Delta P_{tie} \\ \Delta P_{G2} \\ \Delta P_{T2} \\ \Delta f_2 \end{bmatrix}, u = \begin{bmatrix} u_1 \\ u_2 \end{bmatrix}, d = \begin{bmatrix} \Delta P_{d1} \\ \Delta P_{d2} \end{bmatrix}^T$$

$$A = \begin{bmatrix} -\frac{1}{T_{G1}} & 0 & -\frac{1}{R_1 T_{G1}} & 0 & \cdots & 0 \\ \frac{1}{T_{T1}} & -\frac{1}{T_{T1}} & 0 & \cdots & 0 & \\ 0 & K_{p1}\frac{1}{T_{p1}} & -\frac{1}{T_{p1}} & \cdots & 0 & \\ \vdots & \vdots & \vdots & \ddots & \vdots & \\ 0 & 0 & 0 & \cdots & -\frac{1}{R_2 T_{G2}} & \\ 0 & 0 & 0 & \cdots & -\frac{1}{T_{T2}} & \\ 0 & 0 & -a_{12}K_{p2}\frac{1}{T_{p2}} & \cdots & -\frac{1}{T_{p2}} & \end{bmatrix},$$

$$B^T = \begin{bmatrix} \frac{1}{T_{G1}} & 0 & 0 & 0 & 0 & 0 & 0 & 0 \\ 0 & 0 & 0 & 0 & \frac{1}{T_{G2}} & 0 & 0 & 0 \end{bmatrix}$$

$$\delta = \begin{bmatrix} 0 & 0 & -\frac{K_{p1}}{T_{p1}} & 0 & 0 & 0 & 0 \\ 0 & 0 & 0 & 0 & 0 & -\frac{K_{p2}}{T_{p2}} & \end{bmatrix}^T$$

III. Model Based Predictive Control MB PC

MB PC encompasses a variety of control strategies unified by a common concept. The core principle involves forecasting based on a model of the process, which is depicted in Figur 3.

The objective of Model-Based Predictive Control (MBPC) is to forecast the future dynamics of a system within a specified timeframe using a dynamic model and to determine control measures that optimize a given criterion. Typically, this involves minimizing the function J, which is defined as follows:

$$J = \left\{ \sum_{k=n_2}^{n_1} [M(t+k) - Y_m(t+k)] \right\}^2 + \sum_{k=1}^{n_u} \{\lambda (\Delta U_n(t+k))\}^2 \tag{9}$$

In the given control function, $M(k+t)$, $Y_m(k+t)$, and $U_n(k+t)$ represent the predicted process output, the desired reference trajectory, and the control input projected t steps ahead, respectively. n_1 and n_2 denote the minimum and maximum prediction horizons for the process output, while n_u signifies

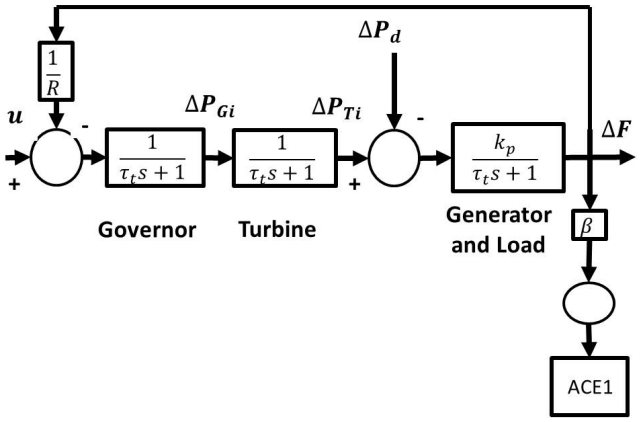

Fig. 1. Schematic representation of the power system for area i.

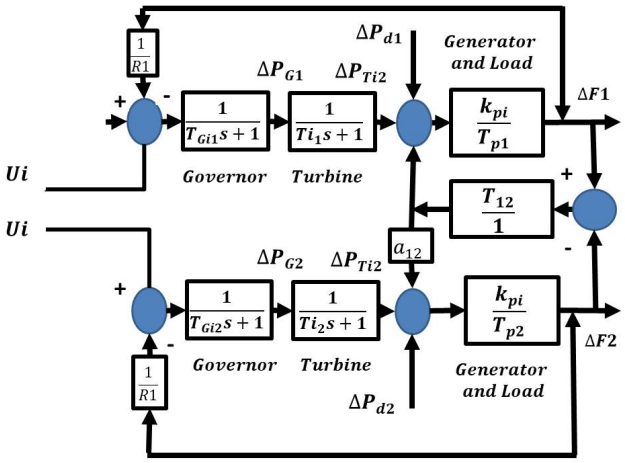

Fig. 2. Two-Area Load Frequency Management Framework.

the control input's prediction horizon. n_2 is chosen to capture the significant portion of the step response curve. Employing a control horizon n_u serves to mitigate the computational intensity of the approach. The factor λ adjusts the influence of the control signal. At each sampling interval, only the initial control action from the computed sequence is enacted on the system. The process is then reiterated at the succeeding sampling instant. This iterative process is referred to as the receding horizon principle. The control architecture is composed of the plant model and an optimization module. The optimization leverages Equation 9 in conjunction with

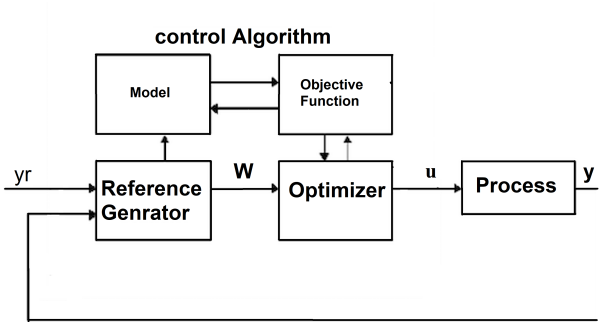

Fig. 3. Traditional Scheme of Model-Based Predictive Control.

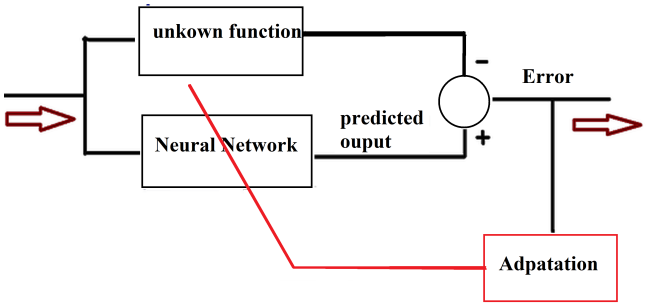

Fig. 4. Neural Network Utilized for Approximating Functions.

constraints on the inputs and outputs.

$$\begin{aligned} u_{\min} \le u_i \le u_{\max}, &\qquad i = 0,\ldots,N_2-1 \\ \Delta u_{\min} \le \Delta u_i \le \Delta u_{\max}, &\qquad i = 0,\ldots,N_2-1 \\ y_{\min} \le y_i \le y_{\max}, &\qquad i = 1,\ldots,N_2 \end{aligned}$$

The capability of MBPC to incorporate constraints is a defining feature that contributes to its widespread adoption, utility, and success in industrial contexts. MBPC techniques are celebrated for their adaptability and resilience in the realm of process control.

IV. Neural Network-Based Predictive Control

Neural networks have been employed with considerable success for the identification and control of dynamic systems due to their universal approximation capabilities. The multilayer perceptron (MLP), in particular, is favored for its effectiveness in modeling nonlinear systems and for the implementation of nonlinear controllers. The process of utilizing a neural network for system modeling is illustrated in Figure 4. Within this context, the unknown function may be associated with the system under control, with the neural network serving as the model for the identified plant. Networks comprising two layers, which utilize sigmoid functions in the hidden layer and linear functions in the output layer, are recognized as universal approximators. The training signal for the neural network is derived from the prediction error between the actual plant output and the neural network's output. This plant model, built on a neural network, leverages historical inputs and outputs to forecast future plant outputs. The configuration of this neural network plant model is detailed in Figure 5. Here, u(t) represents the input to the system, and yp(t) is the predicted output from the plant model.

Using Previous Plant Outputs for Future Predictions with Neural Network Models

The architecture of the neural network model for predicting future plant outputs is outlined in Figure 5. In this setup, $u(t)$ is the input to the system, $y_p(t)$ denotes the actual output of the plant, and $y_m(t)$ represents the output predicted by the neural network model. The model includes tapped delay lines (TDL), which are used to retain previous input values. The weight matrices $\{IW\}^{I,j}$ and $\{LW\}^{i,j}$ correspond to the connections from input j to layer ii and from layer j to layer i, respectively. This neural network can be trained in an offline batch mode using data gathered from the plant's operations. The process of selecting the network parameters is referred to as training the network. The Levenberg–Marquardt (LM) algorithm is particularly effective for this purpose. The LM algorithm is an iterative method designed to find the minimum of a function represented as the sum of squares of nonlinear functions. It is a well-established approach for nonlinear least-squares problems, combining elements of steepest descent and the Gauss–Newton method. The LM algorithm operates in two modes: like a steepest descent method when the current solution is far from the target, ensuring convergence albeit slowly, and like a Gauss–Newton method when the solution is near the target. Assuming a functional relationship f that maps a parameter vector $\mathbf{P} \in \mathbb{R}^m$ to an estimated measurement vector $\hat{\mathbf{x}} = f(\mathbf{p})\mathbf{x}, \hat{\mathbf{x}} \in \mathbb{R}^n$, the goal is to refine the parameter estimate $\mathbf{P}$ to minimize the squared distance $\mathbf{e}^T\mathbf{e}$ with $\mathbf{e} = \mathbf{x} - \hat{\mathbf{x}}$. The LM algorithm uses a linear approximation of f near $\mathbf{P}$, employing a Taylor series expansion for small changes $\delta\mathbf{p}$, leading to $f(\mathbf{P}+\delta\mathbf{p}) \approx f(\mathbf{P}) + \mathbf{J}\delta\mathbf{p}$ where $\mathbf{J}$ is the Jacobian matrix. Through iterative steps, starting from an initial estimate $\mathbf{p}_0$, the algorithm generates a sequence of vectors converging towards a local minimizer $\hat{\mathbf{p}}$ for f. Each step involves solving a linear least-squares problem to find the $\delta\mathbf{p}$ that minimizes $\mathbf{e} - \mathbf{J}\delta\mathbf{p}$.

In the context of the Levenberg–Marquardt (LM) algorithm, the product $\mathbf{J}\delta\mathbf{p} - \mathbf{e}$ is orthogonal to the column space of the Jacobian matrix $\mathbf{J}$. This orthogonality condition leads to the equation $\mathbf{J}^T(\mathbf{J}\delta\mathbf{p} - \mathbf{e}) = \mathbf{0}$, which results in deriving $\delta\mathbf{p}$

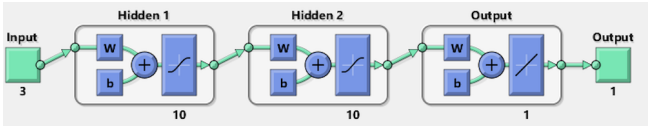

Fig. 5. Configuration of the Plant Model Based on Neural Networks.

as the solution of the normal equations:

$$J^T J \delta_p = J^T e \tag{10}$$

Here, the matrix $\mathbf{J}^T\mathbf{J}$ on the left side of the equation represents the approximate Hessian matrix, essentially an estimation of the matrix of second-order derivatives. However, the LM method slightly modifies this equation, leading to what is known as the augmented normal equations:

$$N\delta_p = J^T e \tag{11}$$

In these augmented equations, the off-diagonal elements of $\mathbf{N}$ match those in $\mathbf{J}^T\mathbf{J}$, while the diagonal elements are defined as $N_{ii} = \mu + [\mathbf{J}^T\mathbf{J}]_{ii}$, where $\mu > 0$, is a positive value. This alteration of the diagonal elements of $\mathbf{J}^T\mathbf{J}$ introduces damping into the system, with μ being the damping term. The process involves updating the parameter vector $\mathbf{p}$ with $\delta\mathbf{p}$ computed from the normal equations. If this update results in a reduction in the error $\mathbf{e}$, it is accepted, and the procedure is repeated with a reduced damping term. Conversely, if the error does not decrease, the damping term is increased. The augmented normal equations are then solved again, continuing iteratively until a value of $\delta\mathbf{p}$ is found that reduces the error. This iterative adjustment is key to the algorithm's ability to converge effectively to a solution. Adjustment of Damping in the Levenberg–Marquardt Algorithm and Termination Criteria In the Levenberg–Marquardt (LM) algorithm, the damping term is finely tuned during each iteration to ensure a consistent reduction in the error e. The algorithm concludes its process when any of the following criteria are met: The iterative process is terminated when one of the following conditions is met:

1. The gradient of $e^T e$ (represented by $\mathbf{J}^T\mathbf{e}$ on the right-hand side of Equation 10 falls below a predetermined threshold ε_1.
2. The relative change in the magnitude of $\delta\mathbf{p}$ becomes lesser than a specified threshold ε_2.
3. The error $e^T e$ itself dips below a set threshold ε_3.
4. The process reaches a predefined maximum number of iterations, $k_{\max}$.

In cases where a covariance matrix Σ for the measured vector $\mathbf{x}$ is accessible, the solution is obtained by addressing a weighted least squares problem, as defined by the weighted normal equations:

$$\mathbf{J}^T\Sigma^{-1}\mathbf{J}\delta\mathbf{p} = \mathbf{J}^T\Sigma^{-1}\mathbf{e} \tag{12}$$

Regarding model predictive control utilizing neural network models for single-input, single-output systems, there have been a limited number of studies, as detailed in reference [27]. For multivariable systems, a strategy employing three fixed multilayer perceptron (MLP) models is described in reference [28]. In our approach, this strategy is adapted to two MLP models with an additional adaptive model, as depicted in Figure 6.

V. Fuzzy Logic Control Strategy

Fuzzy Logic Control (FLC) mimics the decision-making process of a human operator by modulating the input signal based solely on the system's output. This approach to control involves three key stages: fuzzification, the implementation of fuzzy control rules, and defuzzification, as illustrated in Figure 7. The process of designing a fuzzy logic load frequency controller involves using specific input signals.

The aim of this control strategy is to regulate terminal frequency at the output of each area and reduce the discrepancy between actual and reference Area Control Error (ACE). The block diagrams illustrating Load Frequency Control (LFC) with the proposed Neural Network Model Predictive Control (NN-MPC) and Fuzzy Logic Control (FLC) are presented in Figures 9 and 10, respectively. For the proposed system, the cost function as described in Equation 9 is modified to:

TABLE I. Fuzzy Logic Control Protocols for Frequency Deviation

ΔACE/$d\Delta$ACE	LN	MN	SN	Z	SP	MP	LP
LN	LP	LP	LP	MP	SP	Z	-
MN	LP	MP	MP	SP	Z	SN	-
SN	LP	MP	SP	Z	SN	MN	-
Z	MP	SP	Z	SN	MN	MN	-
SP	MP	Z	SN	MN	MN	LN	-
MP	SP	SN	MN	MN	LN	LN	-
LP	Z	SN	MN	LN	LN	LN	-

The cost function is defined as:

$$J = \sum_{k=n_1}^{n_2} k\left(\mathrm{ACE}(t+k) - \mathrm{ACE}_{\mathrm{pred}}(t+k)\right)^2 + \lambda\Delta\mathrm{ACR}_{\mathrm{ref}}(t+k)^2 \quad \text{where} \tag{13}$$

$$\Delta\mathrm{ACR}_{\mathrm{ref}} = \mathrm{ACR}_{\mathrm{ref}}(t+k) - \mathrm{ACR}_{\mathrm{ref}}(t+k-1) \tag{14}$$

Fig. 6. Strategy for Multivariable Neural Network Model Predictive Control (NN-MPC)

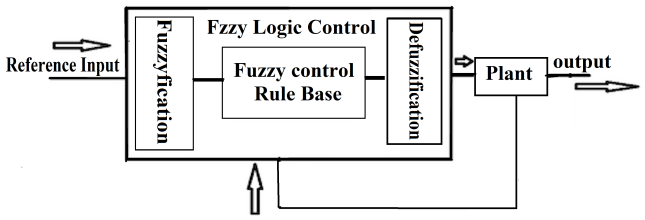

Fig. 7. Tripartite Structure of a Fuzzy Logic Controller.

Constraints are set such that the area output frequency and tie-line power are normalized to 1, correlating to output frequency and tie-line power. Thus, the control input *uu* is constrained by:

$$ACR_{ref} - \varepsilon \leq u \leq ACR_{ref} + \varepsilon \tag{15}$$

Abbreviations:

- LN: Large Negative
- MN: Medium Negative
- SN: Small Negative
- Z: Zero
- SP: Small Positive
- MP: Medium Positive
- LP: Large Positive

VI. 7. Results and Simulation

A controller utilizing a neural network model for forecasting future LFC responses and potential control actions was developed. An optimization algorithm, based on Equation 12, computes control signals to enhance future plant performance. The neural network plant model was trained using the Levenberg–Marquardt algorithm with data derived from the LFC model . The model predictive control method employed was grounded in the receding horizon principle, where the neural network predicts the plant response over a designated time horizon. These predictions inform a numerical optimization program to determine the control signal that best minimizes the performance criterion over this horizon. Implementation of the controller was carried out in Matlab/Simulink, with the following constraint and parameter settings:

$$N_1 = [1,1], \qquad N_2 = [7,6],$$
$$N_u = [2,3], \qquad \lambda = [0.05, 0.08].$$

The state constraints were set to ensure that signals remain within physically plausible ranges, specified as:

$$X_{\min}\mathbf{I}_3 \leq \begin{bmatrix} \Delta f_1 \\ \Delta f_2 \\ \Delta f_3 \end{bmatrix} \leq X_{\max}\mathbf{I}_3$$

he boundaries for the state variables are defined as follows:

$$x_{\min} = \begin{bmatrix} -0.05 \\ -0.05 \\ -0.03 \end{bmatrix}, \quad x_{\max} = \begin{bmatrix} 0.05 \\ 0.05 \\ 0.03 \end{bmatrix}$$

Comparative analysis has been conducted to assess the responses of the power system under the control of the fuzzy logic controller versus the proposed Neural Network Model Predictive Control (NN-MPC). The system parameters under investigation are detailed as follows:

- Nominal frequency (f_0) is 60 Hz,
- Speed regulation constants (R_1 and R_2) are 2.4 Hz per unit MW,
- Governor time constants (T_{G1} and T_{G2}) are set at 0.08 seconds,
- Turbine time constants (T_{T1} and T_{T2}) are set at 0.3 seconds,
- Frequency bias coefficients (B_1 and B_2) are 0.4 MW/Hz,
- Power system time constants (T_{p1} and T_{p2}) are 20,
- Synchronizing coefficient between the two areas (a_{12}) is -1,
- Power system gains (K_{p1} and K_{p2}) are 120,
- Synchronizing power coefficient (T_{12}) is 0.545 MW.

Figure 11 illustrates the response in frequency deviation for Area 1 following a 0.05 per unit (p.u.) load change in Area 1, comparing the performance of the Fuzzy Logic Control (FLC) with that of the proposed Neural Network Model Predictive Control (NN-MPC) in a two-area power system. Figure 12 presents the analogous frequency deviation response for Area 2 resulting from the same disturbance in Area 1 under both control methods. Figure 13 depicts the deviation in tie-line power prompted by a 0.05 p.u. load change in Area 1, showcasing the effects of employing FLC and the proposed NN-MPC. Figure 14 demonstrates the frequency deviation in Area 1 due to a 0.05 p.u. load disturbance in Area 2 when

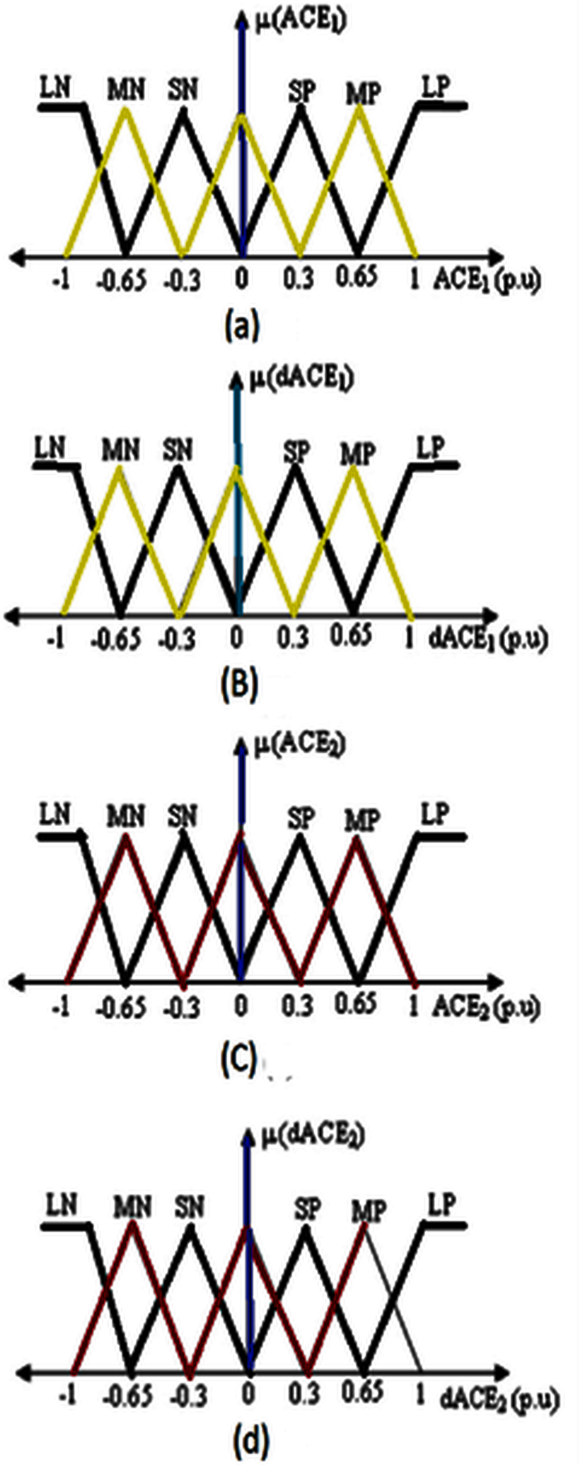

Fig. 8. Membership Functions: (a) Control Error in Area One, (b) Fluctuation of Control Error in Area One, (c) Control Error in Area Two, and (d) Fluctuation of Control Error in Area Two.

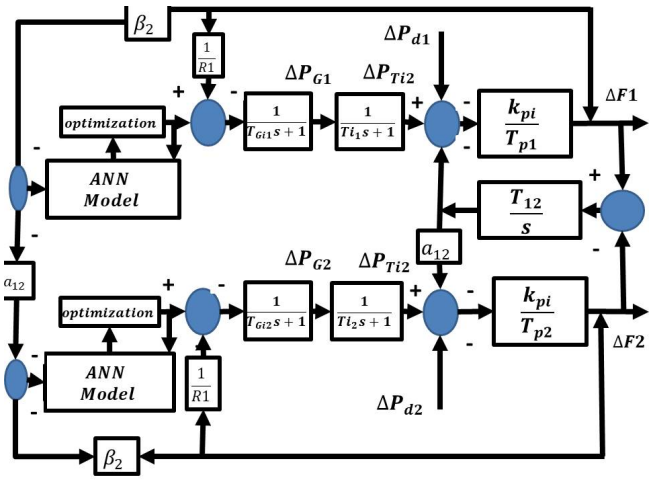

Fig. 9. The Proposed Neural Network Model Predictive Control for the Two-Area Load Frequency Regulation in Power Systems.

both areas are managed by FLC and proposed NN-MPC, with an additional consideration of a 30% increase in the values of regulators R_1 and R_2. Similarly, Figure 15illustrates the frequency deviation response in Area 2 owing to a 0.05 p.u. load disturbance in Area 2 under both control strategies, also with the regulators increased by 30%. Additionally, this figure presents the tie-line power deviation response for the same disturbance and control settings. Table II provides a comparison of the maximum overshoot (max. O.S.) and the settling time (T_s) for the system responses under the FLC and the proposed NN-MPC configurations.

TABLE II. DISTURBANCE IN AREA 1 AND AREA 2 WITH PI

Parameter	Area 1 with PI		Area 2 with PI	
	T (s)	Max (p.u)	T(s)	Max (p.u)
Δf_1	4.8	0.024	15	0.026
Δf_1	5.2	0.006	13	0.008
Δf_2	3.9	0.013	14.5	0.014

TABLE III. DISTURBANCE IN AREA 1 AND AREA 2 WITH NN-MPC

Parameter	Area 1 (NN-MPC)		Area 2 (NN-MPC)	
	Max (p.u.)	Ts (s)	Ts (s)	Max (p.u.)
Δf_1	0.013	2.8	14	0.012
Δf_2	0.014	3.2	12	0.0012
ΔP_{tie}	0.0009	2.9	14	0.015

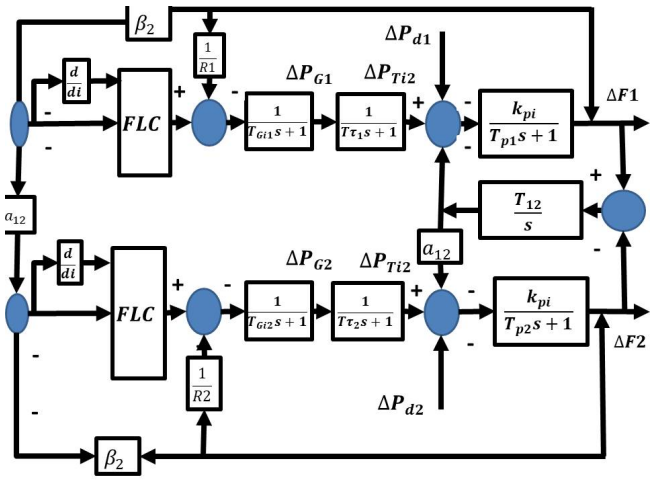

Fig. 10. Schematic Representation of Fuzzy Logic Control for Two-Area Load Frequency Regulation in Power Systems.

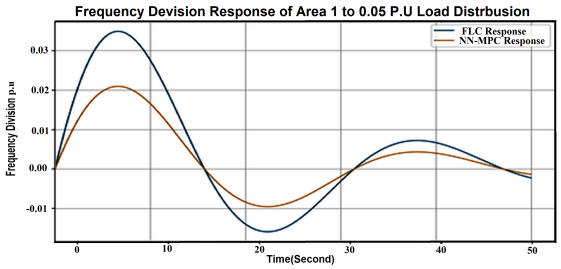

Fig. 11. Response to Frequency Deviation in Area 1 Resulting from a 0.05 p.u. Load Disturbance in a Two-Area Power System Using FLC and NN-MPC.

VII. Explanation and Discussion

This study has developed a matrix of fuzzy rules for the fuzzy logic controller, incorporating 49 rules using triangular membership functions. Additionally, a Neural Network Model Predictive Control (NN-MPC) system has been designed and optimized based on the power system model, as well as control and prediction horizons. Comparative analyses of various transient response curves, including Δf_1, Δf_2, and $\Delta P_{\text{tie-line}}$, have been conducted. Key observations (refer to Figure 16) include:

1. The frequency deviation responses, as illustrated in Figurs 11–16 and summarized in Table 2, indicate that the NN-MPC outperforms fuzzy logic control in terms of quicker response and reduced maximum overshoot.

2. The tie-line power declines more rapidly with the NN-MPC compared to FLC.

3. As depicted in Figs. 11–16 and Table II, the NN-MPC efficiently mitigates mechanical oscillations within 3 seconds.

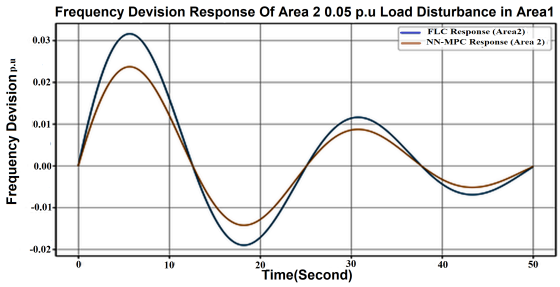

Fig. 12. Response to Frequency Deviation in Area 1 Resulting from a 0.05 p.u. Load Disturbance in a Two-Area Power System Using FLC and NN-MPC.

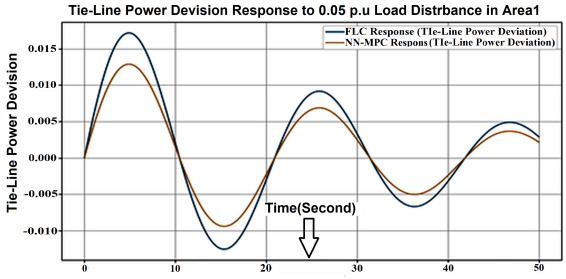

Fig. 13. Response of Area 2 to Frequency Deviation Arising from a 0.05 p.u. Load Disturbance in Area 1 of a Two-Area Power System, Utilizing FLC and NN-MPC.

4. Conversely, the performance of the FLC, shown in the same figures and table, reveals its limited effectiveness in damping mechanical oscillations within 16 seconds.

5. For accurate predictions of the power plant's future behavior, the prediction horizon should exceed the system's oscillation period.

6. The NN-MPC has proven successful in managing several large-scale nonlinear control challenges, making it a superior choice for power system stabilization.

TABLE IV. Disturbance Parameters in Area 1 and Area 2 with FLC

Parameter	Area 1 (FLC)		Area 2 (FLC)	
	Max (p.u.)	T (s)	T (s)	Max (p.u.)
Δf_1	0.012	4.4	4.2	0.022
Δf_2	0.015	5.1	5.2	0.005
ΔP_{tie}	0.0009	3.6	3.5	0.012

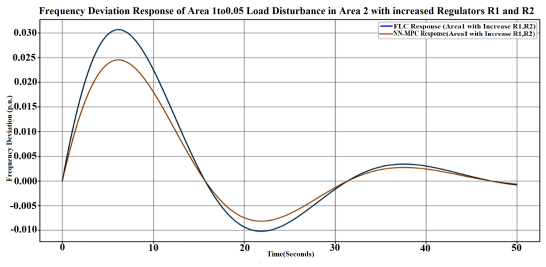

Fig. 14. Frequency Deviation Response in Area 1 Triggered by a 0.05 p.u. Load Disturbance in Area 2 of the Two-Area Power System, Employing FLC and NN-MPC with an Enhanced Setting of Regulators R1 and R2.

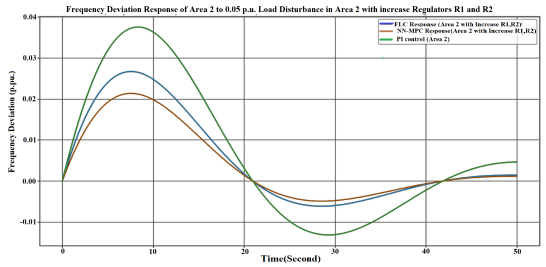

Fig. 15. Frequency Deviation in Area 1 due to 0.05 p.u. Load Change in Area 2.

VIII. Conclusions

This study explores the enhancements that can be realized by applying neural predictive strategies to load frequency control in a two-area interconnected power system. The efficacy of the proposed neural Network Model Predictive Control (NN-MPC) is demonstrated through a comparative analysis with a Fuzzy Logic Controller (FLC). Both controllers were evaluated under load disturbances within the LFC framework. The simulation results indicate that the proposed NN-MPC controller exhibits robustness, with superior transient and steady-state responses, and maintains performance despite variations in system parameters. Furthermore, the simulations suggest that the proposed NN-MPC outperforms the fuzzy logic controller in terms of control efficacy.

Conflict of Interest

The authors have declared no conflict of interest.

Acknowledgment

The authors wish to express their sincere gratitude to the University of Sfax for its invaluable support throughout the duration of this research. The facilities and resources provided have been instrumental in the successful completion of this work.

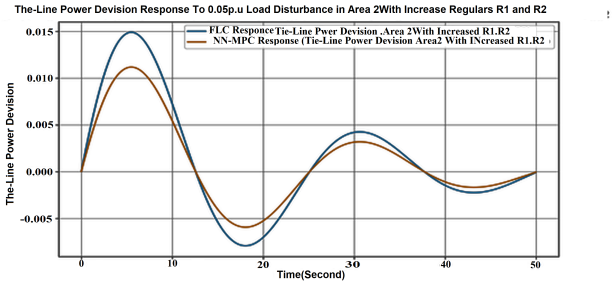

Fig. 16. Frequency Deviation in Area 1 due to 0.05 p.u. Load Change in Area 2.

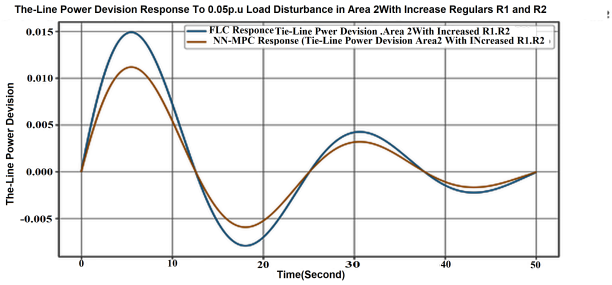

Fig. 17. Response of Tie-Line Power Deviation to a 0.05 p.u. Load Disturbance in Area 2 of a Dual-Area Power System, Utilizing FLC and Enhanced NN-MPC with a 30 Uplift in Regulators R1 and R2.

References

[1] N. Kumari, A. S. Gill, and M. Singh, "Two-area power system load frequency regulation using anfis and genetic algorithm," in *undefined*, 2023. [Online]. Available: https://doi.org/10.1109/INCET57972.2023.10170037.

[2] G. Z. Cao, X. Zhang, P. Li, F. Li, Y. Liu, and Z. Hu, "Load frequency regulation of multi-area power systems with communication delay via cascaded improved adrc," *Energy Reports*, 2023. [Online]. Available: https://doi.org/10.1016/j.egyr.2023.04.379.

[3] S. D. Al-Majidi, M. K. AL-Nussairi, A. J. Mohammed, A. M. Dakhil, M. F. Abbod, and H. S. Al-Raweshidy, "Design of a load frequency controller based on an optimal neural network," *Energies*, vol. 15, no. 17, p. 6223, 2022. [Online]. Available: https://doi.org/10.3390/en15176223.

[4] S. Murali, K. Abhinav, R. Shankar, and S. K. Parida, "Application of deep learning technique based load forecast for frequency regulation," 2022. [Online]. Available: https://doi.org/10.1109/GlobConET53749.2022.9872420.

[5] Y. Wang, X. Chu, Y. Chen, and X. Long, "Research on distributed load regulation optimization based on artificial intelligence," 2023. [Online]. Available: https://doi.org/10.1117/12.2680828.

[6] G. Zhang, M. Teng, S. Chen, and Z. Bie, "A deep reinforcement learning based framework for power system load frequency control," 2022. [Online]. Available: https://doi.org/10.1109/ICPSAsia55496.2022.9949649.

[7] A. Maurya, H. Khan, and H. Ahuja, "Performance of load frequency control of two-area power system by using proportional integral derivative controller," 2023. [Online]. Available: https://doi.org/10.1109/SPIN57001.2023.10117171.

[8] M. Y. Yousef, M. A. Mosa, and A. M. A. Ghany, "Load frequency control for power system considering parameters variation using parallel distributed compensator based on takagi-sugino fuzzy," *Electric Power Systems Research*, 2023. [Online]. Available: https://doi.org/10.1016/j.epsr.2023.109352.

[9] J. H. Lanker, R. Bhushan, N. S. Choudhary, and M. A. Gupta, "Load frequency control of multi area power system using meta-heuristic/artificial intelligence techniques," 2022. [Online]. Available: https://doi.org/10.1109/ICICCSP53532.2022.9862473.

[10] B. S. Rameshappa and N. M. Shadaksharappa, "An optimal artificial neural network controller for load frequency control of a four-area interconnected power system," *International Journal of Power Electronics and Drive Systems*, vol. 12, no. 5, pp. 4700–4711, 2022. [Online]. Available: https://doi.org/10.11591/ijece.v12i5.pp4700-4711.

[11] N. Aziz, M. Abdulrhman, and S. I. Khalel, "Multi area load frequency control using fuzzy type-2," 2022. [Online]. Available: https://doi.org/10.1109/ICECET55527.2022.9872625.

[12] Y. Zheng, J. Tao, Q. Sun, H. Sun, Z. Chen, and M. Sun, "Deep reinforcement learning based active disturbance rejection load frequency control of multi-area interconnected power systems with renewable energy," *Journal of The Franklin Institute-engineering and Applied Mathematics*, 2022. [Online]. Available: https://doi.org/10.1016/j.jfranklin.2022.10.007.

[13] A. Maurya, H. Khan, A. K. Rai, and H. Ahuja, "Load frequency control by using different controllers in multi-area power system networks," 2022. [Online]. Available: https://doi.org/10.1109/ICACRS55517.2022.10029090.

[14] H. Jaber, A. H. Miry, and K. A. Al-Anbarri, "Load frequency control of interconnected power system using artificial intelligent techniques based fractional order piλ dμ controller," *Nucleation and Atmospheric Aerosols*, 2022. [Online]. Available: https://doi.org/10.1063/5.0066839.

[15] S. P. Sebhatu, "Planning of load frequency control in two degrees of freedom pid controller using mfo technique in 2 area power system," 2023. [Online]. Available: https://doi.org/10.1007/978-981-99-0969-8_6.

[16] Y. Zheng, Z. Huang, J. Tao, H. Sun, Q. Sun, M. Dehmer, M. Sun, and Z. Chen, "Power system load frequency active disturbance rejection control via reinforcement learning-based memetic particle swarm optimization," *IEEE Access*, 2021.

[17] J. Sophia, M. Magdalin, and K. Thenmalar, "Fuzzy logic based load frequency control of power system," *Materials Today: Proceedings*, 2021.

[18] D. V. Doan, K. Nguyen, and Q. V. Thai, "A novel fuzzy logic based load frequency control for multi-area interconnected power systems," *Engineering, Technology & Applied Science Research*, 2021.

[19] N. K. Gupta, M. K. Kar, and A. K. Singh, "Load frequency control of two-area power system by using 2 degree of freedom pid controller designed with the help of firefly algorithm." undefined, 2021.

[20] A. D. Shakibjoo, M. Moradzadeh, S. Z. Moussavi, and L. Vandevelde, "A novel technique for load frequency control of multi-area power systems," *Energies*, vol. 13, 2020.

[21] M. Abouheaf, W. Gueaieb, and A. M. Sharaf, "Load frequency regulation for multi-area power system using integral reinforcement learning," *IET Generation, Transmission & Distribution*, 2019.

[22] B. S. R and M. S. Nagaraj, "Load frequency control of two-area interconnected power system using optimal

controller, pid controller and fuzzy logic controller." undefined, 2020.

[23] P. O. Oluseyi, K. M. Yellowe, T. Akinbulire, O. M. Babatunde, and A. S. Alayande, "Optimal load frequency control of two area power system." undefined, 2019.

[24] A. Kumar, N. Anwar, and R. Kumar, "Load frequency regulation using linear active disturbance rejection control technique." undefined, 2020.

[25] X.-C. Shangguan, C.-K. Zhang, L. Jiang, and M. Wu, "Load frequency control of time-delayed power system based on event-triggered communication scheme," *Applied Energy*, 2022.

[26] Z. Wu, P. Li, Y. Liu, D. Li, and Y. Chen, "Optimized cascaded pi controller for the load frequency regulation of multi-area power systems with communication delays," *Energy Reports*, 2022.

[27] D. Sharma, "Automatic generation control of multi source interconnected power system using adaptive neuro-fuzzy inference system." International journal of engineering science and technology, 2020.

[28] R. Mehmet, M. Tur, A. Wadi, A. Shobole, and S. Ay, "Load frequency control of two area interconnected power system using fuzzy logic control and pid controller," in *Proceedings of the IEEE International Conference on Renewable Energy Research and Applications (ICRERA)*, IEEE, 2018.